Available online at http://ijim.srbiau.ac.ir/
Int. J. Industrial Mathematics (ISSN 2008-5621)
Vol. 14, No. 4, 2022 Article ID IJIM-1437, 14 pages
DOI: http://dx.doi.org/10.30495/ijim.2022.20273
Research Article
Science and Research Branch (IAU)

Validation of a Polytropic-Based Blow by Model and Predicting Crevice Flow Cyclic Variations in a CNG SI Engine

E. Abdi Aghdam *†

Received Date: 2020-05-20 Revised Date: 2021-06-06 Accepted Date: 2021-12-13

Abstract

Due to the required clearance between the cylinder liner and piston of a reciprocating IC engine, a few crevices appear among compression rings and cylinder-piston. Although the gas leakage into the crankcase can be controlled substantially via the use of two or three compression rings, it is impossible to remove the existing crevices and the ring orifices of the cylinder-piston-ring pack. Escape of unburned mixture into the crevices can result in a serious impact on the work done per cycle, fuel conversion efficiency, and pollutant emission, which are all important in the firing cycle. In the present work, first a Polytropic-Based Blowby Model (PBBM) was validated using a Thermodynamic Simulation Code (TSC) equipped with a blowby sub-model. Then, using the experimental results extracted from a single-cylinder SI research engine in skip-fire and NG fuel mode, the $P-\theta$ of an Ensemble Average Cycle (EAC) was calculated from the $P-\theta$s of 200 experimental cycles. The crevice flow rates of the EAC were estimated using TSC and PBBM. The results showed a good agreement between them. The study of blowby in 200 experimental cycles via the use of PBBM revealed that the existing cyclic variations of the cylinder pressure caused corresponding cyclic changes in Net Cylinder Mass Lost (NCML) and Net Mass Passed (NMP) through the ring orifices and the pressure inside the crevices. A linear correlation was observed between maximum NCML and cylinder peak pressure while an inverse correlation was detected between cylinder peak pressure and NCML at the EVO position.

Keywords : Blowby, Polytropic; Cyclic variation; Thermodynamic model; CNG; SI engine.

1 Introduction

During the compression and combustion-expansion strokes of the in-cylinder charge, there is aconsiderable pressure difference between the cylinder and the crankcase at any crank angle position. This condition can lead to a serious leakage of the cylinder content. Although the gas leakage toward the crankcase can be controlled substantially by using two or three compression rings, it is impossible to remove the existing crevices and the ring orifices of the cylinder-piston-ring pack. Escape of unburned mixture into the crevices can result in a serious impact on the work done per cycle, fuel conversion effi-

*Corresponding author. eaaghdam@uma.ac.ir, Tel:+98(45)31500000.
†Department of Mechanical Engineering, Faculty of Engineering, University of Mohaghegh Ardabili, Ardabil, Iran.

Abbreviation			
Symbol			
A	Cross section area	bTDC	Before top dead center
C	Constant, Celsius	CA	Crank angle
C_d	Discharge coefficient	CC	Correlation coefficient
m	Mass	CNG	Compressed natural gas
P	Pressure	EAC	Ensemble average cycle
R	Ideal gas constant	EVO	Exhaust valve open
T	Temperature	FBRC	Free burned residual-gas cycle
t	Time	IC	Internal combustion
V	Volume	IT	Ignition timing
γ	Specific heat ratio	IVC	Inlet valve close
λ	Relative air-fuel ratio	NCML	Net cylinder mass lost
θ	Crank angle	NG	Natural gas
Subscript		NMP	Net mass passed
i	Counter	ODE	Ordinary differential equation
max	Maximum	PBBM	Polytropic-based blowby model
R1& R2C	Crevice between first and second rings	R1	First compression ring
u	Unburned	R2	Second compression ring
Super-script		SI	Spark ignition
$^\circ$	Degree	TDC	Top dead center
Acronym		TLC	Top land crevice
aBDC	After bottom dead center	TSC	Thermodynamic simulation code
aTDC	After top dead center		
bBDC	Before bottom dead center		

ciency, and the emission of pollutants, which are all important in a firing cycle. Therefore, the estimation of the mass exchange between the cylinder and the connected crevices plays a crucial role in determining the performance and emissions of a SI engine.

Ting and Mayer [1] used a volume-orifice model to estimate the pressure behind the rings in their cylinder wear study. Namazian and Haywood [2] used this theory to evaluate hydrocarbonpollutants emitted from SI engines. Havas and Muneer [3] developed a semi-empirical model tocalculate the flow rate of leaking gases from an internal combustion engine. With the development of a computer program, they showed that by increasing the number of rings fromthree to five, the blowby rate decreased. They also concluded that the blowby flow rate had ahyperbolic function with the number of rings. Kouremenos et al. [4] investigated the effects ofvarious parameters such as blowby rate and compression ratio on a direct-injection diesel engineat cold and hot motoring conditions. Using the peak pressure value, they showed that as the peak pressure value occurring before TDC increased, the blowby rate also increased. Koszalka and Niewczas [5] experimentally studied the effect of the crevice volume between rings on blowby and oil consumption. They adjusted the amount of free space between the rings by modifying the highest ring groove height and found that increasing the amount of the crevice volume caused a significant increase in the oil consumption. Abdi Aghdam and Kabir [6] investigated the crevice flow in a two-stroke research engine under motoring condition using a thermodynamic model associated with a blowby sub-model based on a volume-orifice theory. Their results showed an excellent agreement between the experimental pressure data and the thermodynamic model at the three tested com-

pression ratios of 7.6, 10.2, and 12.4. They also showed in their study that the maximum cylinder mass lost occurred at about 4°CAaTDC and increased by the increase of compression ratio.

In the motoring mode, the mass exchange rate has been predicted and validated through a blowby sub-model coupled to an engine thermodynamic model [6, 7, 8]. Since it is more difficult toaccurately simulate the practical cycles in the code, it is impossible to predict the mass exchangeof different cycles in SI engines. The blowby sub-model, which is used to predict the mass exchange rate between the cylinder, the connected cylinder-ring-piston crevices, and the crankcase, is often investigated based on a volume-orifice theory [2, 6, 7, 8, 9]. Centered on the theory, Abdi Aghdam and Tahouneh [8] developed a Polytropic-Based Blowby Model (PBBM) in their study on the blowby phenomenon of some experimental, fueled motoring cycles. To validate the result of the model, they defined the output $P-\theta$ of an SI engine Thermodynamic Simulation Code (TSC) equipped with a blowby sub-model as the input to PBBM. Then they compared the predictions of PBBM with those of the TSC. Finding a good agreement between the two sets of results, they concluded that the PBBM is capable of predicting the crevice flows of experimental cycles.

Irimescu et al. [10] studied the relationship between blowby rate and compression ratio in atransparent SI engine based on pressure. In line with fuel-air ratio estimations using an oxygensensor in the exhaust system, they found that the mass lost was significantly dependent on the compression ratio and the engine speed. Gargate et al. [11] developed a formula for calculating blowby by practical tests on three heavy-duty diesel engines using simulation and classification parameters affecting blowby. The amount of leakage obtained by this formula was in good agreement with the experimental data. Malagi [12] estimated the multi-cylinder diesel engine blowby by meshing a model through a finite element and applying appropriate boundaries according to the engine operating conditions and considering the lubrication effect around the piston. They found that much of the gas flow leaked through the ring orifice. The results of their blowby model turned out to be in good agreement with the experimental results.

Koszalka and Guzik [13] presented a mathematical model for cylinder-ring-piston sealing in an internal combustion engine based on the volume-orifice theory and ring displacement and torsion in piston grooves. They considered the thermal deformation of the ring, piston, and cylinder as well as the heat transfer between the gas flowing through the orifices and the surrounding walls in their calculations.

It has been emphasized that the leakage of unburned mixture into the crevices can have a serious impact on cycle work, fuel conversion efficiency, and engine pollutant emissions. It isparticularly important to check the PBBM in the firing condition because the in-cylinder pressure in this mode is much higher than that of the motoring mode. Also, the model can be simply used for any experimental cycle. The purpose of the present work is first to verify the PBBM using a thermodynamic simulator equipped with a blowby sub-model, then to estimate the actual cycle blowby through the model, and finally, to examine cyclic variations in the crevice flows caused by the in-cylinder pressure cyclic changes.

2 Thermodynamic SI engine code

Based on temporal and temporal-spatial attention to in-cylinder flow field, mathematical modelsof SI engines are divided into two basic thermodynamic (based on the first and secondthermodynamic laws) and multidimensional (fluid dynamics-based) models. Since themultidimensional models require very high computational power, they are inconvenient for thecases with high-level iteration computations (such as design cases). Some researchers prefer touse these models only in motoring conditions to obtain flow field history in the complex enginegeometries. In addition, the low accuracy of these models necessitates the attainment of a good, balanced accuracy in all sub-models, since low-accuracy sub-

models lead to the development of low-accuracy models, which cannot be appropriate for the applications requiring high levels of accuracy [14]. In the present work, a thermodynamic model is utilized to verify the PBBM. In thermodynamic models, the first law of thermodynamics plays a key role in the incremental process used. In these models, in-cylinder charge is divided into several zones each with uniform temperature, pressure, and composition. In a multi-zone model, the number of zones is more than one, usually burned and unburned zones, and they are separated by a surface termed 'flame front'. In such models, the flame propagation is controlled by a function or turbulent burning velocity expression. Temperature and pressure in both burned and unburned regions are assumed to be uniform with no heat exchange between them. The composition of the unburned gases is generally assumed to be constant and the burned gas composition is assumed to be in a thermochemical equilibrium. Blizard and Keck [15] introduced an eddy entrainment model assuming homogeneous eddy volumes. They hypothesized that the entrained vortices are burned under laminar burning velocity by the diffusion transportation of radicals between adjacent eddies over a characteristic time. The models are often referred to as "entrainment models", which have the advantage of being compatible with the flame observation techniques such as natural light and Schlieren. These models are accompanied by two differential equations: one for the entrained mass and the other for the burned mass. Several thermodynamic models have been established and developed using the turbulent entrainment and eddy burn-up bases [16, 17, 18, 19, 20, 21, 22]. In the present work, a thermodynamic code developed in Leeds-Ardabil [23] has been employed.

3 Blowby sub-model

As mentioned above, blowby sub-models which are used to predict mass exchange between the cylinder, crankcase, and cylinder-ring-piston crevice flows are often established on the volume-orifice theory. Various objectives have been considered for the use of this sub-model, such as predicting the amount of the unburned hydrocarbons [2], the durability of the ring-bush pack [1], and the effects of blowby on the combustion process in the cylinder [7, 23]. In this theory, it is assumed that several volumes, including cylinder, crevices, and crankcase, are connected in series through interlocking orifices in a way that if there is a pressure difference between two volumes, mass flow occurs from the high pressure volume to the low pressure one through the common orifice. Fig. 1 shows the configuration of these volumes for two compression-ring mode.

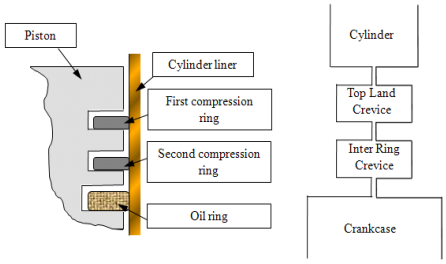

Figure 1: Volume-orifice simulation model of two compression-ring systems.

In most ignition engines, for shortening the combustion period and preventing the engine knock,the spark plug is located near the cylinder head and mainly inclined to the cylinder axis tominimize its distance from the end-gas inside the cylinder. With this idea, even during thecombustion process, the in-cylinder unburned zone is connected to Top Land Crevice (TLC). As the flame propagates to the cylinder-crevice border, the cylinder pressure increases and approaches its maximum value before consuming all in-cylinder unburned mixture. After the occurrence of peak pressure, the unburned mixture in the TLC can flow back into the cylinder due to negative pressure difference. If the combustion process follows the above procedure, the burned mixture will not enter to the TLC during the flame propagation. As a result, it can be assumed that only the unburned mixture is exchanged between the cylinder and TLC. Thus, it is predicted that the mass flow rate through the orifices can be estimated using the blowby sub-model and its geometry.

In the compression stroke, as the piston moves,

the cylinder pressure rises and its gas flows into the TLC. TLC pressure increases and its pressure difference with the inter-ring crevice causes a flow from the first ring (R1) orifice. With the appearance of the pressure difference between the inter-ring crevice and the crevice between the second compression-ring (R2) and the oil-ring, which is almost widely connected to the crankcase space, the possibility of mass flow through R2 orifice is realized. The downstream direction is maintained until the peak pressure of the cylinder occurs. However, the flow direction can be changed depending on the pressure difference between the volumes.

The flow through an orifice depends on the pressure difference between its two sides [24]. The mass flow rate through the orifice between volumes i and $i+1$ is determined by the pressure ratio as follows:

If $P_{i+1} \prec P_i$, the orifice flow direction will be from volume i to volume $i+1$, which can be expressed by the following two states:

[(a)]If $\frac{P_i}{P_{i+1}} \prec \left(\frac{\gamma_i+1}{2}\right)^{\frac{\gamma_i}{(\gamma_i-1)}}$, the mass flow rate is obtained from the Eq. (3.1),

$$\frac{dm_{i,i+1}}{dt} = C_d A_{i,i+1} \left[\frac{2\gamma_i}{(\gamma_i-1)RT_i}\right]^{\frac{1}{2}} \left(\frac{P_{i+1}}{P_i}\right)^{\frac{1}{\gamma_i}} \left[1-\left(\frac{P_{i+1}}{P_i}\right)^{\frac{(\gamma_i-1)}{\gamma_i}}\right]^{\frac{1}{2}} P_i \quad (3.1)$$

where C_d, $A_{i,i+1}$, and γ_i are the discharge coefficient, orifice cross section area, and the specific heat ratio in ith volume, respectively. If $\frac{P_i}{P_{i+1}} \succ \left(\frac{\gamma_i+1}{2}\right)^{\frac{\gamma_i}{(\gamma_i-1)}}$, the flow is chocked and the mass flow rate is determined from Eq.(3.2),

$$\frac{dm_{i,i+1}}{dt} = C_d A_{i,i+1} \left[\frac{\gamma_i}{RT_i}\right] \left(\frac{2}{\gamma_i+1}\right)^{\frac{(\gamma_i+1)}{2(\gamma_i-1)}} P_i \quad (3.2)$$

2.

Due to a higher surface to volume ratio of the crevices, the gas temperature inside the crevices can be fixed at a value equal to the wall temperature. Assuming that the gas within the crevices obeys the ideal gas law, the ith volume pressure rate resulting from the mass flow rates can be expressed as Eq. (3.2),

$$\frac{dP_i}{dt} = \frac{RT_i}{V_i}\left(\frac{dm_{i-1,i}}{dt} - \frac{dm_{i,i+1}}{dt}\right) \quad (3.3)$$

Supposing that cylinder and crankcase pressures are known, two equations can be obtained from the development of Eq. (3.3) for the two crevices. The time-based equations can be easily converted to crank angle-based equations using the engine speed, which is summarized as follows:

$$\frac{d}{d\theta}\begin{pmatrix}P_2\\P_3\end{pmatrix} = \begin{pmatrix}f_1[\theta,P_1,P_2,P_3,P_4]\\f_2[\theta,P_1,P_2,P_3,P_4]\end{pmatrix} \quad (3.4)$$

which is a first order Ordinary Differential Equation (ODE) system where P_1, P_2, P_3, and P_4 are the cylinder, TLC, inter-ring crevice, and crankcase pressures, respectively. The equation was solved in the model using second order Runge-Kutta method. During the current study, the blowby-related geometric dimensions, such as the cylinder and piston diameters, ring cross section and gap, ring grave, and location on piston land were measured at ambient temperature. Then the dimensions were corrected to the estimated wall temperature using the thermal expansion coefficients of the engine materials [6]. Finally, the TLC and inter-ring crevice volumes and the orifice cross section areas were calculated. Table 1 illustrates the required dimensions used in the blowby sub-model.

4 Polytropic-based blowby model

The Polytropic-Based Blowby Model (PBBM) has previously been studied for the prediction of cylinder mass lost in the motoring (free combustion) cycle and validated against a TSC [8]. The cylinder pressure history ($P-\theta$) together with the unburned mixture quality and the cylinder charge temperature at Inlet Valve Closed timing (IVC) were included in the model. First, the cylinder mass at the IVC was evaluated using engine geometry. Then, polytropic index was determined

Table 1: Geometric values used in the blowby sub-model.

Geometric character	**Size**
TLC volume (cm^3)	1.6455
Inter-ring volume (cm^3)	1.1129
TLC cross section area (cm^2)	0.824
First compression ring orifice area (cm^2)	6.1×10^{-3}
Second compression ring orifice area (cm^2)	8.1×10^{-3}

using an incremental change in the cylinder pressure and volume. Finally, in-cylinder temperature was estimated using the polytropic relation of an ideal gas. Given that in the motoring mode, the cylinder unburned mixture is connected to the TLC, the mass flow rate through the orifices can be determined using the blowby sub-model, cylinder and crevice pressures, and blowby geometry. Full details of this model and its validation have been presented in the Ref. [8].

5 Experimental apparatus

In the present work, a single-cylinder SI research engine, modified from a durable diesel-based engine by the GUNT Company, was used. The engine was coupled to an electrical adjustable-speed dynamometer, so that the output power from the engine could be restored to the mains using a recovery unit.

The engine specifications are summarized in Table 2. Fig. 2 shows the schematic diagram and arrangement of the utilized equipment [25]. In the current work, an Adlink DAQ2005 four-channel data logger with a maximum sampling rate of 500 kHz was used to record in-cylinder dynamic pressure, absolute inlet pressure, crank angle, and TDC signals.

In the present study, the sampling frequency was set to 120 kHz so as to record about 8000 samples per cycle at 1800 rpm. A Kistler Type 2613B shaft encoder, fixed to the free-end of the crankshaft, was used. It allowed adjustment of the spark advance and the fuel injection start positions with a one-degree resolution. The in-cylinder pressure was measured by a Kistler 6052C dynamic pressure sensor with high sensitivity and low thermal shock drift. The signal

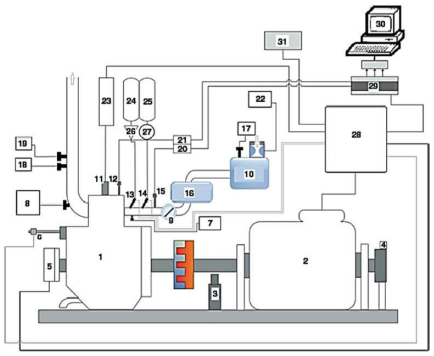

Figure 2: Schematic diagram of the experiment platform including 1. Engine, 2. Dynamometer, 3. Engine speed sensor, 4. Torque sensor, 5. Shaft encoder, 6. Suction TDC sensor, 7. Inlet mixture temperature sensor, 8. Exhaust gas temperature sensor, 9. Throttle, 10. Primary air comfort chamber, 11. Spark plug, 12. Dynamic pressure transducer, 13. NG injector, 14. Gasoline injector, 15. Absolute pressure transducer, 16. Secondary air comfort chamber, 17. Primary comfort tank temperature sensor, 18. Gas analyzer a, 19. Gas analyzer b, 20. Amplifier of the absolute pressure transducer, 21. Amplifier of dynamic pressure transducer, 22. Inlet air flow sensor, 23. Ignition system, 24. NG tank, 25. Gasoline tank, 26. NG pressure regulator, 27. Gasoline pump, 28. Engine management system, 29. AD-Logger, 30. PC, 31. Electricity input of the system [25].

of the sensor was first amplified by a Kistler 5011 amplifier; then it was transmitted to the data logger; and finally, it was recorded by the related software. More details about the utilized measuring devices are presented in Ref. [23].

6 Experimental procedure

After adjusting the compression ratio to 10.0, the engine was run in the firing mode using natural gas as the fuel so as to achieve a warm steady state. The steady state was attained as the oil

Table 2: Specifications of the engine used.

Specification	Description
Cylinder diameter	90 mm
Stroke	70 mm
Compression ratio	10
Spark ignition system	Electrical with 1°CAstep
Fuelling system	Port injection
Cooling system	Single-flow water
Valve number andlocation	2 OHV
Inlet valve timing	Open @ 0°CATDC, close @ 50°CAaBDC
Exhaust valve timing	Open @ 40°CAbBDC,close @ 8°CA aTDC
Chamber type	Disc shaped

and cooling water temperatures stayed at constant values. The engine speed was set at 1800 rpm and the exhaust gas analyzer was activated. The quality of the exhaust products was evaluated by a gas analyzer in terms of the relative air-fuel ratio (λ). According to the (λ), the amount of the injected fuel was adjusted to obtain the desired equivalence ratio and the associated experimental data were recorded. After extracting the raw data through AD-Logger software, the data were processed using a program written in FORTRAN, and then the required analyses were conducted.

7 Procedure of the thermodynamic and polytropic models

From the measurements and experimental results processed for the Free Burned Residual Gas Firing Cycles (FBRCs), the geometry and operating conditions of the engine and the blowby geometric values were first applied to the TSC equipped to a blowby sub-model. By running the TSC, variations of different parameters, such as the pressures in the cylinder and crevices and the net mass passed down through the orifices, in terms of the crank angle were obtained. Then, the same engine operating conditions, the identical geometries (engine and blowby), and the in-cylinder pressure data obtained from the TSC were defined as the inputs to the PBBM. By controlling the inputs and executing the program, the predictions of the model for the blowby features were extracted and the obtained results were compared with the TSC results.

8 Results and discussion

To investigate the blowby prediction of the TSC, the experimental data were extracted from an NG-fueled engine at the compression ratio of 10, the engine speed of 1800 rpm, and the ignition timing of 30° CAbTDC. To lower the number of effective variables such as residual burned gas fraction (affecting temperature, burning velocity, and thermodynamic properties) and eliminate their effects, skip fire technique with seven-cycle repetition period (successive four motoring and three firing cycles) was employed. Under these conditions, the first firing cycle of each period of the data can be considered as FBRC. The next two firing cycles were only intended to keep the engine warm, which is important in the NG-burn state. The raw data of 1400 sequential cycles were extracted at the above conditions. Then, the 200 first-firing cycles were separated and analyzed. Fig. 3 illustrates the in-cylinder pressure versus crank angle for the 200 FBRCs associated with an Ensemble Average Cycle (EAC). It should be noted that from definition, the EAC indicated mean effective pressure (*imep*) is equivalent to the average *imep* of the cycles under investigation.

It can be observed that even under the skip fire mode, the cyclic variations have not beensignificantly reduced, and until the IT, the cycles have

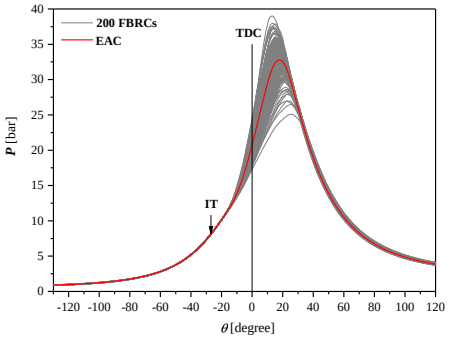

Figure 3: In-cylinder pressure versus crank angle for 200 FBRCs and EAC.

colligated and then split in the combustionperiod. After applying the required geometries and setting up the engine operation condition, the TSC was run and in-cylinder pressure was estimated. Fig. 4 depicts the $P-\theta$ predicted by the TSC and the $P-\theta$ of the experimental EAC along with their relative deviation. Although the difference between the two $P-\theta$ results is noticeable around the peak pressure, the relative deviation is serious in the other parts; however, it is indistinct in the $P-\theta$ diagrams. It can be seen that the maximum deviation is less than 1% until IT and the maximum value in the studied range is about 5% in the combustion period before TDC, which is generally appropriate and acceptable. Therefore, it can be reasoned that there is a good agreement between the cylinder pressures of the TSC and the EAC.

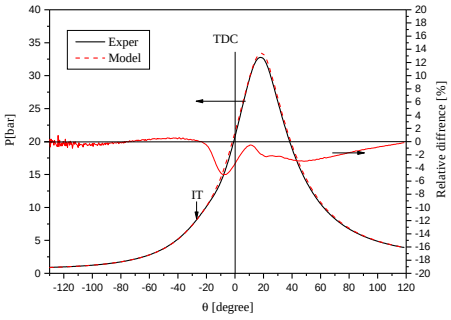

Figure 4: The $P-\theta$ of the EAC and the $P-\theta$ predicted by the TSC along with their relative deviation.

The TSC results for the TLC and inter-ring crevice pressures are shown in Fig. 5. The peak valueof the TLC pressure was about 0.26 bar lower than the cylinder peak pressure value at the samecrank position, while the inter-ring crevice peak pressure appeared at 80°CAaTDC with a value of 5.237 bars. After this position, the inter-ring crevice pressure reduced due to the net mass flow from the relevant orifices.

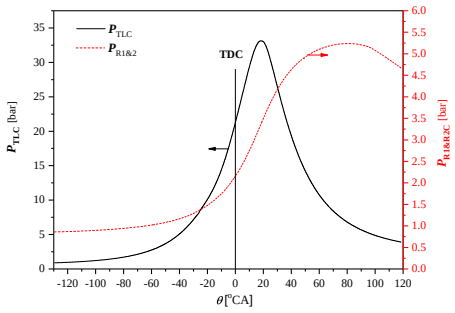

Figure 5: The TSC results for the TLC and inter-ring crevice pressures.

Fig. 6 illustrates Net Cylinder Mass Lost (NCML) and Net Mass Passed (NMP) from the first ring (R1) and second ring (R2) orifices toward the crankcase versus crank angle as the percentage of the cylinder mass at IVC. It can be observed that the NCML reaches a maximum of 13.71% at the peak pressure position, reduces with cylinder pressure drop during piston motion, and approaches about 2.05% at EVO position. The maximum NMP through the R1 orifice is about 1.54% at 96°CAaTDC position. By decreasing the TLC pressure (PTLC) relative to the pressure of the crevice between R1 and R2 (PR1& R2C), a reverse flow from the R1 orifice occurs and its NMP reaches about 1.5% at EVO. The maximum NMP from the R2 orifice is about 0.48% occurring at the EVO position. This passed mass has no chance of returning to the cylinder through the crevice flow.

As mentioned earlier in the PBBM, the blowby sub-model and geometries are used to estimatecrevice flow. The PBBM inputs are the cycle $P-\theta$, initial conditions, and fuel type. This sub-model predicts the crevice flow via performing relatively low-volume calculations. In the incremental blowby calculations, the cylinder pressure and temperature and the unburned gas specific heat ratio are required. The model incrementally estimates the cylinder temperature using a polytropic behavior of the cylinder unburned gas

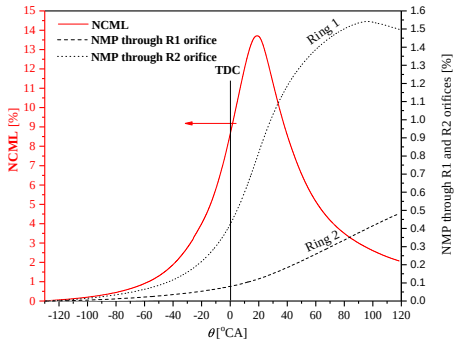

Figure 6: NCML and NMP through R1 and R2 orifices toward the crankcase versus crank angle.

($PV^n = C$). In the present work, the $P - \theta$ obtained from TSC and the initial conditions were applied to the PBBM; then the NCML and NMP from the R1 and R2 orifices were evaluated. Fig. 7 shows the NCML versus crank angle for the TSC and PBBM. Until 60°CAaTDC, a very good agreement can be observed between them with very close maximum values occurring at roughly similar locations.

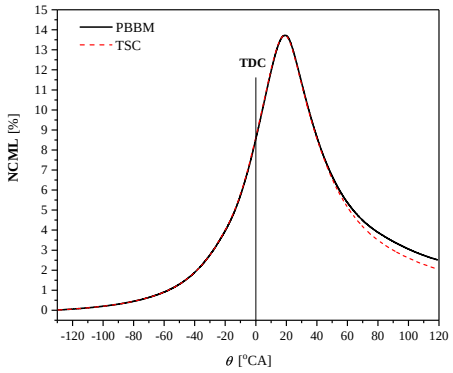

Figure 7: NCML percentage versus crank angle for the TSC and PBBM.

Fig. 8 demonstrates the NMP across the R1 and R2 orifices for the TSC and the PBBMpredictions. In Fig. 8(a), a very good agreement can be observed for the NMP through R1orifice with the maximum value of 1.54% at 95.5∘CAaTDC. As can be seen in Fig. 8(b), the maximum NMP from the R2 orifice is about 0.48% at EVO. The main reason for the good agreement can be the dependency of the crevice flows on the crevice pressure differences, orifice cross-section areas, and crevice volume and temperature, which are all identical in both TSC and PBBM. As mentioned earlier, the main difference is in the in-cylinder unburned gas temperature.

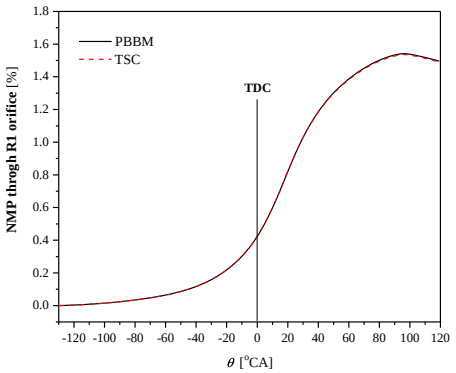

(a)

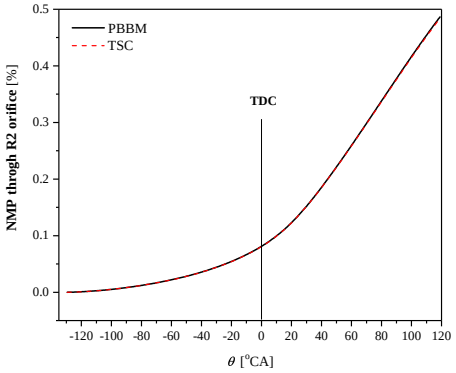

(b)

Figure 8: NCML percentage versus crank angle for the TSC and PBBM.

As noted, the flow through the orifices connecting the assumed crevices with constanttemperature and volume strongly depends on the pressure differences between them. Therefore,it is important to extract pressure changes in the TLC and the crevice between the two rings inthe NCML toward the crankcase by the blowby codes. Shown in Fig. 9 are pressure histories ofthe crevices versus crank angle resulted from the use of TSC and PBBM. A very good agreement can be seen between the results.

The flow speeds in the orifices were estimated from the flow rates and geometries of R1 and R2orifices. Fig. 10 shows the flow speed in terms of crank angle at R1 orifice for the TSC andPBBM. It is well adapted that the flow speed in the range of 78°CAbTDC to 64°CAaTDCremains constant at a maximum value equivalent to the local sound speed.

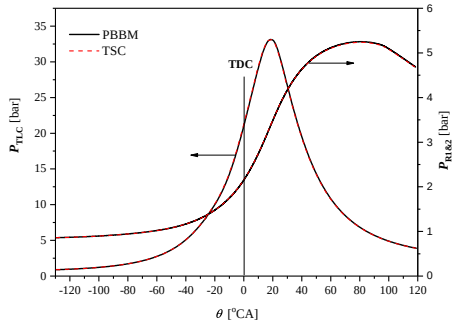

Figure 9: Pressure histories of TLC and the inter-ring crevice versus crank angle for TSC and PBBM.

Choking phenomenonprevents the increase of mass flow rate. The speed becomes zero at 95.5°CAaTDC when NMP through R1 orifice reaches maximum value (Fig. 8a). The following negative speed indicates a change in the flow direction. Fig. 11 illustrates the flow speed from the R2 orifice with a good adaptation, continued by a maximum value or choked speed from 20°CAbTDC up to EVO.

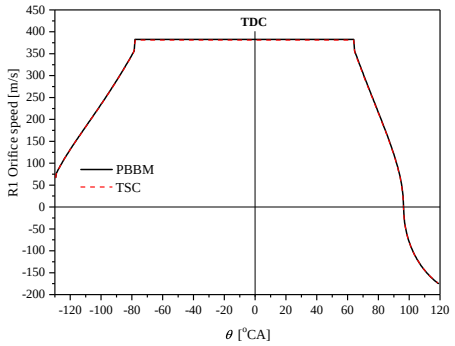

Figure 10: Flow speed at the R1 orifice versus crank angle for the TSC and PBBM.

In the PBBM, the in-cylinder unburned mixture temperature is determined from the corresponding equations. In the TSC, heat transfer to the walls is simulated, but heat exchangebetween the burned and unburned zones is ignored even if unburned gas enters in the entrainedflame front. Fig. 12 demonstrates the unburned gas temperature versus crank angle predicted bythe TSC and PBBM. It can be seen that the temperature difference is not serious up to30°CAaTDC; after that in the TSC, it decreases due to the above reasons and reaches thecylinder wall temperature (80°C in the current study). Although in this period, the in-cylinderunburned gas mass fraction is not significant, it is the main source for the deviations of the NCMLs in TSC and PBBM appearing at crank angles higher than 50°CAaTDC.

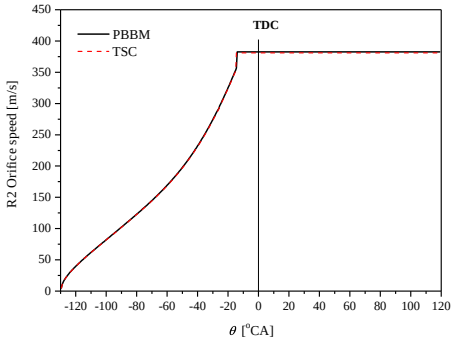

Figure 11: The R2 orifice speed versus crank angle for the TSC and PBBM.

Based on the comparative results and the good agreement between the PBBM and TSC, it can beconcluded that the PBBM can predict the crevice flow without following complex thermodynamic calculations.

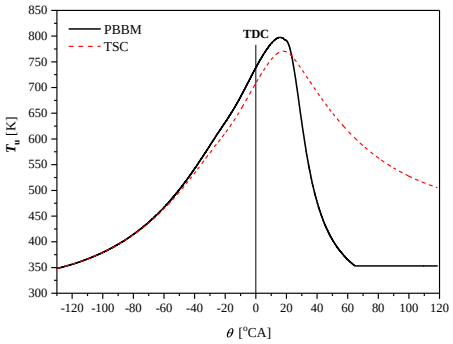

Figure 12: In-cylinder unburned gas temperatures versus crank angle Predicted by TSC and PBBM.

To investigate the blowby predictions of PBBM for practical cycles, 200 first firing cycles from the experimental data of the skip fire mode with seven-cycle period (shown in Fig. 3) were analyzed. The individual $P - \theta$ data of the experimental cycles and that of the EAC were defined as the input to the PBBM with known initial conditions. Fig. 13 represents the NCML versus crank angle for the experimental cycles and EAC. Significant similarity can be observed between Fig. 13 and Fig. 3 emphasizing a close relationship between cylinder pressure and NCML. To deter-

mine this relationship, the maximum NCMLs in terms of the cylinder peak pressures of the cycles were examined. Fig. 14 indicates the maximum NCML against peak pressure for the 200 FBRCs. A linear dependency can be seen between the maximum NCML and cylinder peak pressure with a linear fit of $NCML_{\max}(\%) = 0.78819 + 0.38446P_{\max}$ and a correlation coefficient of 0.9997. The linear relationship indicates that for a one bar increase in the peak pressure, the maximum NCML increases by about 0.385%.

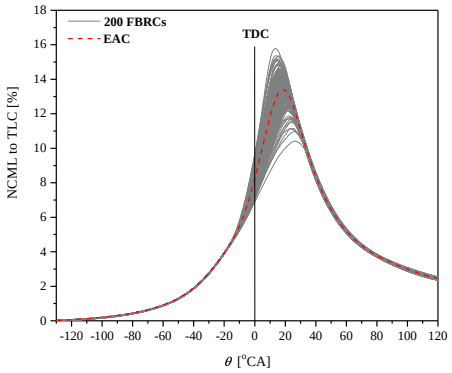

Figure 13: NCML to TLC for 200 FBRCs and EAC.

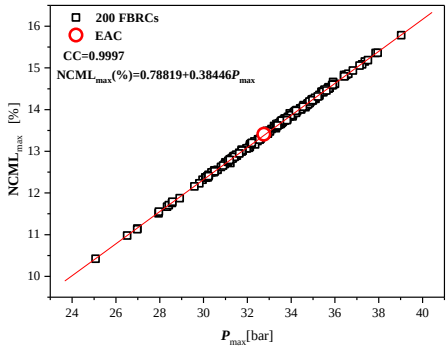

Figure 14: Maximum NCML versus cylinder peak pressure for 200 FBRCs and EAC.

Due to the lake of flame and lower burned gas temperature at EVO, the NCML at this position does not have a good opportunity to burn. That is why the returned unburned mass after EVO is important from hydrocarbon (HC) emission point of view. Fig. 15 indicates the NCML at EVO position in terms of peak pressures for 200 experimental cycles and the EAC. A general inverse dependency can be seen between this NCML and the peak pressure, and the linear fit between them yields a correlation coefficient of 0.8745. When the peak pressure of a cycle in a test is higher than the other, its main combustion length is shorter because IT is constant. During the expansion stroke after peak pressure position, cylinder pressure commences to drop due to the work and heat transfers so that for a cycle with higher peak pressure, the pressure drop integration until EVO can be larger. To clarify the behavior, Fig. 16 indicates in-cylinder pressure at EVO versus the peak pressure for the 200 FBRCs and the EAC.

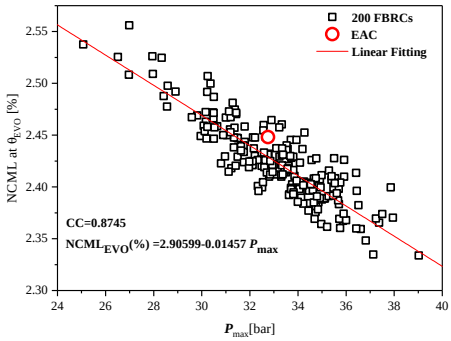

Figure 15: NCML at EVO versus peak pressure for 200 FBRCs and EAC.

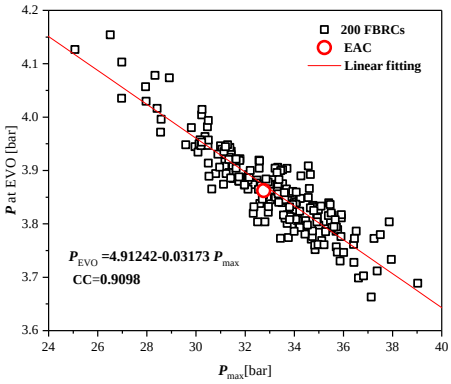

Figure 16: Cylinder pressure at EVO in terms of peak pressure for 200 FBRCs and EAC.

At EVO position, the dependency of NCML and cylinder pressure was considered for the 200 FBRCs and the EAC. Fig. 17 shows NCML versus cylinder pressure at EVO for the 200 experimental cycles and the EAC. A direct relationship can be seen with a linear fitting leading to a correlation coefficient of 0.9399. It should be noted that the unburned mass returning to the cylinder

after EVO is not useful for the cycle; it either results in an incomplete combustion or is left as the unburned gas. As a result, it can increase the amount of pollutant emissions.

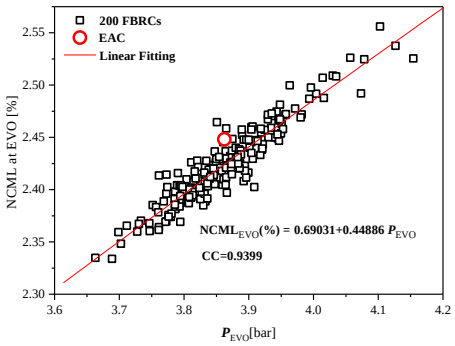

Figure 17: NCML versus cylinder pressure at EVO for 200 FBRCs and EAC.

9 Conclusion

From the different stages of the present study, a few conclusions were extracted, which are summarized below. In first stage, the validation of PBBM via the use of TSC was pursued and the following results were obtained:

- The outputs of the TSC and PBBM showed that NCML increased with the increase of cylinder pressure, reached its maximum level at the peak pressure position, and decreased with the decrease of cylinder pressure.
- A very good agreement was observed between the crevice flow results of PBBM and TSC. Therefore, it can be argued that the PBBM is capable of predicting the cylinder blowby for any experimental cycle without following considerable thermodynamic calculations.
- Using the EAC extracted from 200 FBRCs in the IVC to EVO period (-130 to 120°CA), the PBBM predicted the maximum values of 13.7%, 1.54%, and 0.48% for NCML at the peak pressure position, NMP across R1 orifice at 95.5°CAaTDC, and NMP through R2 orifice at EVO position, respectively.
- The results showed that there was no significant pressure difference between cylinder and TLC due to a relatively larger cross section area between them. However, the pressure difference between TLC and the inter-ring crevice was found to be considerable, and the inter-ring peak pressure was predicted to be about 5.25 bars at 80$\hat{c}irc$CAaTDC.
- From the mass exchange between volumes due to the pressure differences, flow speedsthrough the orifices were estimated. The results showed that the chocking phenomenon was the main reason for the reduction of the mass lost to the crankcase. For the R1 orifice, the chocking range was from 78°CAbTDC to 64°CAaTDC while for the R2 orifice the chocking started from 20$\hat{c}irc$CAbTDC and continued to the EVO position.

After verification, the PBBM was applied to 200 experimental firing cycles recorded in skip fire mode during the current study. From the application of the model, the following results were obtained:

- There was a linear correlation between the maximum NCML to TLC and the cylinder peakpressure with a correlation coefficient of 0.9997. A linear fitting indicated that for each bar of increase in the peak pressure, maximum NCML increased by about 0.385%.
- An inverse general correlation was observed between cylinder peak pressure and NCML at EVO position, and linear fitting between them yielded a correlation coefficient of 0.8745.
- At EVO position, linear behavior was observed between the NCML and the cylinder pressure, and the coefficient of determination was found to be 0.9098.
- In some dependency checking, the EAC did not settle down on the overall behavior fitting ofthe experimental cycles.

- This model is capable of predicting blowby crevice flow for any experimental cycle using engine and blowby geometries and initial conditions.

- Using this model, it is possible to get an in-depth look at crevice flow cyclic variations arising from in-cylinder pressure changes caused by cyclic combustion.

- This model can be used to properly evaluate hydrocarbon emission and develop any parameters related to cylinder pressure history such as mass fraction burned and heat release rate in an SI engine.

References

[1] L. L. Ting, J. E. Mayer, Piston Ring Lubrication and Cylinder Bore Wear Analysis, Part 1 - Theory, *Journal of Lubrication Technology* (1974) 305-314.

[2] M. Namazian, J. B. Heywood, Flow in the Piston-Cylinder-Ring Crevices of a Spark-Ignition Engine: Effect on Hydrocarbon Emissions, Efficiency and Power, *SAE Paper*, 820088, 1982.

[3] M. M. Havas, T. Muneer, Mathematical model for calculating the blowby rate, *Energy Conversion and Management* 21 (1981) 213-218.

[4] D. A. Kouremenos, C. D. Rakopoulos, D. T. Hountalas, The maximum compression pressure position relative to top dead centre as an indication of engine cylinder condition and blowby, *Energy Conversion and Management* 35 (1994) 857-870.

[5] G. Koszalka, A. Niewczas, Influence of top ring axial clearance on oil consumption in diesel engine, *KONES Internal Combustion Engine* 10 (2003) 437-442.

[6] E. Abdi Aghdam, M. M. Kabir, Validation of blowby model using experimental results in motoring condition with the change of compression ratio and engine speed, *Experimental Thermal and Fluid Science* 34 (2010) 197-209.

[7] E. Abdi Aghdam, Improvement and validation of a thermodynamic S.I. engine simulation code, *PhD Thesis, Department of Mechanical Engineering, University of Leeds*, 2003.

[8] S. Tahouneh, E. Abdi Aghdam, Validation of a Polytropic-Base Blowby Model using Experimental Data of Gasoline Fuelled Motoring Cycles, *Modares Mechanical Engineering* 17 (2017) 205-212 (in Persian).

[9] E. Abdi aghdam, A. Zamzam, Study of the Effect of Engine Speed and the Operating life on Blowby in Fueled Motoring for XU7JP/L3 Engine, *Journal of Mechanical Engineering*, 2019; 48(**??**): 209-218. (In Persian)

[10] A. Irimescu, C. Tornatore, L. Marchitto, S. S. Merola, Compression ratio and blowby rates estimation based on motored pressure trace analysis for an optical spark ignition engine, *Applied Thermal Engineering* 61 (2013) 101-109.

[11] S. Gargate, R. Aher, R. Jacob, S. Dambhare, Estimation of blowby in dieselengine: case study of a heavy duty diesel engine, *Emerging Engineering Research and Technology* 2 (2014) 165-170.

[12] R. R. Malagi, Estimation of blowby in multicylinder diesel engine using finite element approach, *SAE International* 2012-01-0559, 2012.

[13] G. Koszalka, M. Guzik, Mathematical model of piston ring scoling in combustion engine, *Polish Mari Time Research* 21 (2014) 66-78.

[14] I. Arsie, C. Pianese, G. Rizzo, Models for the Prediction of Performance and Emissions in a Spark Ignition Engine, *A Sequentially Structured Approach.; SAE paper* 980779, 1998.

[15] N. C. Blizard, J. C. Keck, Experimental and Theoretical Investigation of Turbulent Burning Model for Internal Combustion Engines; *SAE paper* 740191, 1974.

[16] RJ. Tabaczynski, CR. Ferguson, K. A. Radhakrishnan turbulent entrainment model for spark-ignition engine combustion, *SAE International, papernr* 770647, 1977.

[17] S. Merdjani, CGW. Sheppard, Gasoline engine cycle simulation using the Leeds turbulent burning velocity correlations, *SAE International, papernr*, 932640, 1993.

[18] S. Verhelst, R. A. Sierens, A quasi-dimensional model for the power cycle of a hydrogen-fuelled ICE, *Int. J. Hydrogen Energy* 32:3545-54, 2007.

[19] S. Verhelst, C. Sheppard, Multi-zone thermodynamic modelling of spark-ignition engine combustion–an overview, *Energy Conversion and management* 50 (2009) 1326-1335.

[20] Perini Federico, Paltrinieri Fabrizio, Mattarelli Enrico, A quasi-dimensional combustion model for performance and emissions of SI engines running on hydrogen-methane blends, *Int. J. Hydrogen Energy* 35 (2010) 4687-701.

[21] Anand M. Shivapuji, S. Dasappa, Quasi dimensional numerical investigation of syngas fuelled engine operation: MBT operation and parametric sensitivity analysis, *Applied Thermal Engineering* 124 (2017) 911-928.

[22] J. Vancoillie, L. Sileghem, S. Verhelst, Development and validation of a quasi-dimensional model for methanol and ethanol fueled SI engines, *Applied Energy* 132 (2014) 412-425.

[23] M. Sarabi, Simulation and development and validation of dual-fuel (Gasoline-Natural gas) thermodynamic multi zone SI engine code using experimental results obtained from CT300 research engine, *University of Mohaghegh Ardabili, PhD thesis, Jan.* 2020.

[24] JB. Heywood, Internal combustion engine fundamentals, *New York: McGraw-Hill*; 1988.

[25] M. Sarabi, E. Abdi Aghdam, Experimental analysis of in-cylinder combustion characteristics and exhaust gas emissions of gasoline–natural gas dual-fuel combinations in a SI engine, *Journal of Thermal Analysis and Calorimetry* 6 (2020) 3165-3178, http://dx.doi.org/10.1007/s10973-019-08727-2./

Ebrahim Abdi Aghdam is a Professor Faculty member of University of Mohaghegh Ardabili in Faculty of Engineering, Department of Mechanical Engineering. He received his Ph.D. from University of Leeds, UK in 2001. His research interests include modelling and experimental investigations in the field of spark ignition engines.